AIMS Mathematics, 7(10): 17785–17801.
DOI: 10.3934/math.2022979
Received: 03 April 2022
Revised: 07 July 2022
Accepted: 12 July 2022
Published: 03 August 2022

http://www.aimspress.com/journal/Math

Research article

The NHRS scheme for the Chaplygin gas model in one and two dimensions

Kamel Mohamed[1,2], **Hanan A. Alkhidhr**[3] **and Mahmoud A. E. Abdelrahman**[1,4,*]

[1] Department of Mathematics, College of Science, Taibah University, Al-Madinah Al-Munawarah, Saudi Arabia
[2] Department of Mathematics, Faculty of Science, New valley University, New Valley, Egypt
[3] Department of Mathematics, College of Science, Qassim University, Buraidah, Saudi Arabia
[4] Department of Mathematics, Faculty of Science, Mansoura University, Mansoura 35516, Egypt

* **Correspondence:** Email: mahmoud.abdelrahman@mans.edu.eg.

Abstract: The main motive of this work is to introduce a numerical investigation for the one and two-dimensional (1D/2D) Chaplygin gas model. Namely, we developed the non homogeneous Riemann solver (NHRS) method to solve these models. After discussing the Chaplygin gas models and the numerical scheme, various 1D and 2D test problems are introduced. In order to complete the numerical investigation in a completely unified way, Rusanov scheme, modified Lax-Friedrichs and analytical solution are compared with NHRS scheme in 1D case. The acquired results clarify the high resolution of the NHRS technique. The NHRS technique is efficacious and robust. Finally, our study displays that the NHRS scheme is a very powerful tool to solve many other models arising in applied science.

Keywords: hyperbolic conservation laws; Chaplygin gas model; NHRS scheme; Riemann problem; high order accuracy
Mathematics Subject Classification: 35L65, 35L67, 65M08, 76M12, 76N15, 35Q35

1. Introduction

Nonlinear hyperbolic systems of conservation laws play the important roles in building mathematical models for many natural processes in applied science and new physics. Some examples include gas dynamics used in aerospace engineering, equations of nonlinear elasticity, ultra-relativistic Euler equations, Chaplygin gas model, phonon-Bose model, blood flow via arteries, traffic flow, multiphase flow, among other. The analytical investigates of these non-linear models with the aid of mathematical modeling is a cumbersome task. Recently, the numerical simulations have become so vital tools for better understanding of such models [1–5]. There are so many flow fields involving wave phenomena are reflected in nonlinear hyperbolic of coupled nonlinear equations. One

of the so famous model is the Chaplygin gas model. This model plays a crucial and a vital role in fluids to depict the accelerated expansion of the universe and evolution of the perturbations of energy density.

The Chaplygin gas model is early proposed by Chaplygin [6] as a model in aerodynamics. The Chaplygin gas was considered as a possible equation for dark energy [7]. In [8] Brenier investigated the 1D Riemann problem and introduced solutions with concentration for initial data belong to a certain domain in the phase plane. In [9], Guo et al. neglected this constrain and constructed the global solutions for the 1D Riemann problem, in which δ-shock is emerged. Indeed, the 2D Riemann problem displays the elementary patterns of flow fields. 2D Riemann problems with special initial data that are constant along each ray from the origin, are interesting and vital open problems in the topic of hyperbolic systems of conservation laws. In recent years, there has been much progress in 2D Riemann problems for the compressible Euler equations and some related models, such as isentropic compressible Euler model [10, 11], Chaplygin gas Euler models [12, 13], transport model [14], pressure gradient models [15, 16] and the nonlinear wave model [17].

In the ongoing research, we develop the non homogeneous Riemann solver (NHRS) scheme to solve one and two space dimensional Chaplygin gas models. This method includes predictor; corrector stages. The first stage consists of a parameter of control for numerical diffusion, that is based on Riemann invariants and limiters theory. The second stage recovers the balance conservation equation, see [18–24]. Most standard schemes required Riemann solution to compute the numerical flux. In contrast to these schemes, the NHRS scheme can evaluate the numerical flux in the absence of Riemann solution, which is a very fascinating feature. Indeed, this scheme can be implemented as a box solver for so many other models of conservation laws. We give several numerical test cases to clarify the performance the **NHRS** scheme in 1D and 2D cases. In 1D model, the acquired numerical solutions are compared with Rusanov scheme, modified Lax-Friedrichs scheme and the analytical solution. We also concerned with 2D Riemann problems for the Chaplygin gas model. It was found that **NHRS** scheme is superior over the other schemes. Our results depict that the NHRS scheme is a very robust technique, which can be utilized to solve other models, like phonon-Bose system [3], Ripa model [25], blood flow in human artery [26], etc.

The rest of the framework of this paper is organized as follows: Section 2 presents the essential notions for the Chaplygin gas model. Section 3 introduces the 1D and 2D NHRS scheme to solve the Chaplygin gas models. Section 4 gives various one and two-dimensional numerical test problems in order to examine the processes of formation for the constructed waves. Conclusions and remarks of the present results appear in Section 5.

2. Mathematical models

The one-dimensional (1D) Chaplygin gas model [27] is

$$\begin{aligned} (\rho)_t + (\rho\, u)_x &= 0, \\ (\rho\, u)_t + (\rho\, u^2 + P)_x &= 0, \end{aligned} \tag{2.1}$$

$\rho > 0$ and u refer to density and velocity, where the pressure P is given by the state equation

$$P = -\tfrac{1}{\rho}. \tag{2.2}$$

The 1D Chaplygin gas model is a 2×2 system of conservation law, that can be represented as

$$W_t + F(W)_x = 0, \tag{2.3}$$

where

$$W = \begin{pmatrix} \rho \\ \rho u. \end{pmatrix}, \quad \text{and} \quad F(W) = \begin{pmatrix} \rho u \\ \rho u^2 - \frac{1}{\rho} \end{pmatrix}.$$

System (2.3) can represented in the following quasi linear form

$$\begin{pmatrix} \rho_t \\ u_t \end{pmatrix} + \begin{pmatrix} u & \rho \\ \frac{1}{\rho^3} & u \end{pmatrix} \begin{pmatrix} \rho_x \\ u_x \end{pmatrix} = 0. \tag{2.4}$$

The system (2.1) has eigenvalues

$$\lambda_1 = u - \frac{1}{\rho} \; < \; \lambda_2 = u + \frac{1}{\rho}. \tag{2.5}$$

The corresponding eigenvectors of Eq (2.1) is

$$r_1 = \left(\rho, \frac{-1}{\rho}\right)^T, \;\; r_2 = \left(\rho, \frac{1}{\rho}\right)^T. \tag{2.6}$$

So, model (2.1) is a strictly hyperbolic for $\rho > 0$. Indeed, $\nabla\lambda_i \cdot r_i = 0$, i=1, 2, that imply that λ_1 and λ_2 are linearly degenerate and the associated waves are both contact discontinuities [1]. Hyperbolic systems with linearly degenerate eigenvalues play a crucial role in physics and applied mathematics [28].

We take into account the Riemann problem (RP) for the system (2.1) with the following initial data:

$$W(x, 0) = \begin{cases} (\rho_l, u_l), & \text{if} \quad x < 0, \\ \\ (\rho_r, u_r), & \text{if} \quad x > 0, \end{cases} \tag{2.7}$$

where ρ_l, ρ_r, u_l and u_r are constant distributions.

On the other hand, the two dimensional (2D) Chaplygin gas model can be expressed as:

$$\frac{\partial W}{\partial t} + \frac{\partial \mathbf{F}(\mathbf{W})}{\partial x} + \frac{\partial \mathbf{G}(\mathbf{W})}{\partial y} = 0, \tag{2.8}$$

where $\mathbf{W}$ is the conserved variable, $\mathbf{F}(\mathbf{W})$ and $\mathbf{G}(\mathbf{W})$ are the physical fluxes, which are given by

$$\mathbf{W} = \begin{pmatrix} \rho \\ \rho u \\ \rho v \end{pmatrix}, \mathbf{F}(\mathbf{W}) = \begin{pmatrix} \rho u \\ \rho u^2 + P \\ \rho uv \end{pmatrix}, \mathbf{G}(\mathbf{W}) = \begin{pmatrix} \rho v \\ \rho uv \\ \rho v^2 + P \end{pmatrix}, \tag{2.9}$$

where ρ is the density of gas depth, u and v are the velocities in the x and y directions, whereas P is calculated from state equation (2.2). For more details about the 2D Chaplygin gas model, we refer to [31].

3. Numerical schemes

3.1. The NHRS scheme for 1D problem

In order to derive the NHRS scheme, integrating the Eq (2.3) through $[t_n, t_{n+1}] \times [x_{i-\frac{1}{2}}, x_{i+\frac{1}{2}}]$, yields

$$W_i^{n+1} = W_i^n - \frac{\Delta t}{\Delta x}\left(F\left(W^n_{i+\frac{1}{2}}\right) - F\left(W^n_{i-\frac{1}{2}}\right)\right), \tag{3.1}$$

where $F(W^n_{i\pm\frac{1}{2}})$ is the numerical flux at the interface $x = x_{i\pm\frac{1}{2}}$; time t_n and W_i^n is the space-time of the solution W. To construct the numerical fluxes $F\left(W^n_{i\pm\frac{1}{2}}\right)$ at $x_{i\pm\frac{1}{2}}$, it needs Riemann solution at $x_{i\pm\frac{1}{2}}$. We suppose that the self-similar solution to the RP corresponding to Eq (2.3) with initial condition

$$W(x,0) = \begin{cases} W_L, & \text{if} \quad x < 0, \\ \\ W_R, & \text{if} \quad x > 0, \end{cases} \tag{3.2}$$

is

$$W(x,t) = R_s\left(\frac{x}{t}, W_L, W_R\right),$$

R_s is the Riemann solution that has to be either approximated or exactly. We define the intermediate state $W^n_{i\pm\frac{1}{2}}$ in (3.1) at the cell interface $x = x_{i\pm\frac{1}{2}}$ as follows

$$W^n_{i+\frac{1}{2}} = R_s\left(0, W_i^n, W_{i+1}^n\right). \tag{3.3}$$

This procedure is adapted by the NHRS scheme given in [18–23], for numerical simulation of non homogeneous system in one and two dimensional.

In order to construct $W^n_{i+\frac{1}{2}}$, we integrate the Eq (2.3) again over the domain $[t_n, t_n + \theta^n_{i+\frac{1}{2}}] \times [x^-, x^+]$ that contains $x_{i+\frac{1}{2}}$ as shown in Figure 1.

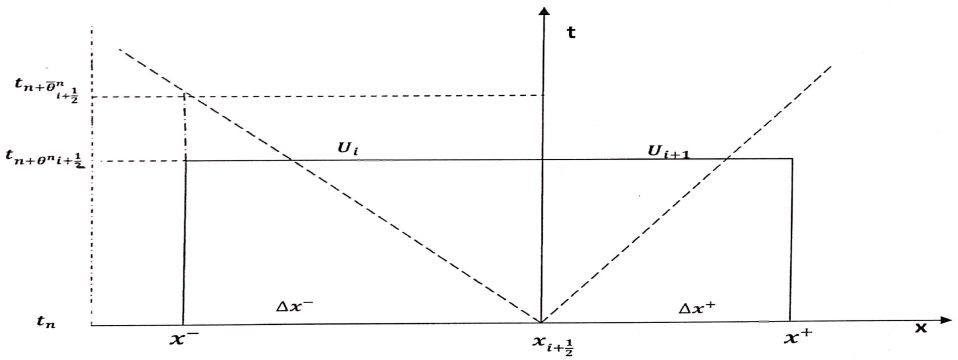

Figure 1. The control space-time domain in the modified Rusanov method.

In general, we will take $x^- = x_i$ and $x^+ = x_{i+1}$, this leads to

$$W^n_{i+\frac{1}{2}} = \frac{1}{2}\left(W_i^n + W_{i+1}^n\right) - \frac{\theta^n_{i+\frac{1}{2}}}{\Delta x}\Big(F(W^n_{i+1}) - F(W^n_i)\Big), \tag{3.4}$$

where $W^n_{i+\frac{1}{2}}$ is an approximate average of the solution W in the control domain $[t_n, t_n + \theta^n_{i+\frac{1}{2}}] \times [x_i, x_{i+1}]$ defined as

$$W^n_{i+\frac{1}{2}} = \frac{1}{\Delta x} \int_{x_i}^{x_{i+1}} W(x, t_n + \theta^n_{i+\frac{1}{2}}) dx. \tag{3.5}$$

In order to complete the implementation of the previous finite volume scheme the time parameter $\theta^n_{i+\frac{1}{2}}$ has to be selected. The selection of the parameter $\theta^n_{i+\frac{1}{2}}$ depends on the stability analysis scheme, see [18], we selected the variable $\theta^n_{i+\frac{1}{2}}$ as the following

$$\theta^n_{i+\frac{1}{2}} = \alpha^n_{i+\frac{1}{2}} \frac{\Delta x}{2S^n_{i+\frac{1}{2}}}, \tag{3.6}$$

where $\alpha^n_{i+\frac{1}{2}}$ is a local parameter to be calculated locally and $S^n_{i+\frac{1}{2}}$ is the local Rusanov velocity defined as

$$S^n_{i+\frac{1}{2}} = \max_{k=1,\dots,K} (\max(|\lambda^n_{k,i}|, |\lambda^n_{k,i+1}|)) \tag{3.7}$$

with$\lambda^n_{k,i}$ is the k-th eigenvalues in (2.5). Then, we can write the predictor stage (3.4) as follows

$$W^n_{i+\frac{1}{2}} = \frac{1}{2}(W^n_i + W^n_{i+1}) - \frac{\alpha^n_{i+\frac{1}{2}}}{2S^n_{i+\frac{1}{2}}} \left[F(W^n_{i+1}) - F(W^n_i)\right]. \tag{3.8}$$

It is clear that $\alpha^n_{i+\frac{1}{2}} = \frac{\Delta t}{\Delta x} S^n_{i+\frac{1}{2}}$ one recovers the Lax-Wendroff method [28] and $\alpha^n_{i+\frac{1}{2}} = 1$ in the linear case the proposed scheme reduces to the classical Rusanov scheme [29] and in the non linear case one recovers first order scheme written as follows

$$\alpha^n_{i+\frac{1}{2}} = \left(1 - \Phi\left(r_{i+\frac{1}{2}}\right)\right) \frac{S^n_{i+\frac{1}{2}}}{s^n_{i+\frac{1}{2}}} + \frac{\Delta t}{\Delta x} S^n_{i+\frac{1}{2}} \Phi\left(r_{i+\frac{1}{2}}\right), \tag{3.9}$$

where $s^n_{i+\frac{1}{2}} = \min_{k=1,\dots,K} (\max(|\lambda^n_{k,i}|, |\lambda^n_{k,i+1}|))$ and $\Phi_{i+\frac{1}{2}} = \Phi\left(r_{i+\frac{1}{2}}\right)$ is an appropriate limiter which is defined by using a flux limiter function Φ acting on a quantity that measures the ratio $r_{i+\frac{1}{2}} = \frac{W_{i+1-q} - W_{i-q}}{W_{i+1} - W_i}$, $q = \text{sign}\left[F'(W^n_{i+\frac{1}{2}})\right]$ of the upwind change to the local change by using Riemann invariants [30]. Finally, we write the modified Rusanov scheme for Eq (2.3) as follows

$$\begin{cases} W^n_{i+\frac{1}{2}} = \frac{1}{2}(W^n_i + W^n_{i+1}) - \frac{\alpha^n_{i+\frac{1}{2}}}{2S^n_{i+\frac{1}{2}}} \left[F(W^n_{i+1}) - F(W^n_i)\right], \\ \\ W^{n+1}_i = W^n_i - r^n \left[F\left(W^n_{i+\frac{1}{2}}\right) - F\left(W^n_{i-\frac{1}{2}}\right)\right]. \end{cases} \tag{3.10}$$

We can write the proposed scheme with non uniform grids as follows

$$\begin{cases} W^n_{i+\frac{1}{2}} = \frac{h_i W^n_i + h_{i+1} W^n_{i+1}}{h_i + h_{i+1}} - \frac{\alpha^n_{i+\frac{1}{2}}}{2S^n_{i+\frac{1}{2}}} \left[F(W^n_{i+1}) - F(W^n_i)\right], \\ \\ W^{n+1}_i = W^n_i - r_i \left[F(W^n_{i+\frac{1}{2}}) - F(W^n_{i-\frac{1}{2}})\right], \end{cases} \tag{3.11}$$

with $r_i = \frac{\Delta t}{h_i}$.

3.2. Well-balanced NHRS scheme for 2D problem

We integrate Eq (2.8) on a generic control volume c_i, that result from the discretization of the computational domain into a number of control volume

$$\int_{c_i} \left(\frac{\partial W}{\partial t} + \frac{\partial F(W)}{\partial x} + \frac{\partial G(W)}{\partial y} \right) dx\, dy = 0,$$

from the divergence theorem, we obtain the following

$$\int_{c_i} \frac{\partial W}{\partial t}\, dx\, dy + \int_{\delta c_i} \Big(F(W)n_x + G(W)n_y \Big)\, d\sigma = 0.$$

Let $\mathcal{F}(W, \vec{n}) = F(W)n_x + G(W)n_y$ and suppose that W_i is constant per cell (mean value of W in the cell c_i). So, we obtain

$$A_i \frac{\partial W_i}{\partial t} + \sum_{j \in K(i)} \int_{\gamma_{ij}} \mathcal{F}(W, \vec{n}) d\sigma = 0,$$

where A_i is the area of the cell c_i and $K(i)$ is the set of neighboring triangles of the cell c_i, with $\vec{n} = (n_x, n_y)^t$ is the unit outward normal to the surface δc_i. Following similar formalism as in 1D, we can define the numerical flux as follows

$$\int_{\gamma_{ij}} \mathcal{F}(W, \vec{n})\, d\sigma = \phi(W_i^n, W_j^n, \overrightarrow{n_{ij}}) mes(\gamma_{ij}),$$

where $mes(\gamma_{ij})$ is the length of the edge γ_{ij}.

Finally, we can write the corrector stage of the scheme in the following form:

$$W_i^{n+1} = W_i^n - \frac{\Delta t_n}{A_i} \sum_{j \in K(i)} \phi(W_i^n, W_j^n, \vec{n_{ij}}) mes(\gamma_{ij}), \tag{3.12}$$

with $\phi(W_i^n, W_j^n, \vec{n_{ij}})$ is the two dimensional numerical flux.

Our goal here is to write the numerical flux similar to the one-dimensional case. We can write

$$\phi(W_i^n, W_j^n, \vec{n}_{ij}) = \mathcal{F}(W_{ij}^n, \vec{n}_{ij}),$$

where W_{ij}^n is determined at the predictor stage. To determine the W_{ij}^n , we project Eq (2.8) on the local outward normal η and tangential $\eta^\perp$.

We get

$$\begin{cases} \dfrac{\partial \rho}{\partial t} + \dfrac{\partial \rho U}{\partial \eta} = 0, \\ \dfrac{\partial \rho U}{\partial t} + \dfrac{\partial (\rho U^2 + P)}{\partial \eta} = 0, \\ \dfrac{\partial \rho V}{\partial t} + \dfrac{\partial \rho UV}{\partial \eta} = 0, \end{cases} \tag{3.13}$$

where $U = \vec{V} \cdot \eta = un_x + vn_y$ and $V = \vec{V} \cdot \eta^\perp = -un_y + vn_x$ are the normal and tangential velocity respectively, we can write the predictor stage using $M_{ij}(X) = \frac{1}{2}(X_i + X_j)$ and $\Delta_{ij}(X) = X_j - X_i$ as follows:

$$\begin{cases} (\rho)_{ij} = M_{ij}(\rho) - \dfrac{\alpha^n_{ij}}{2S^n_{ij}}\Delta_{ij}(\rho U), \\ (\rho U)_{ij} = M_{ij}(\rho U) - \dfrac{\alpha^n_{ij}}{2S^n_{ij}}\Delta_{ij}(\rho U^2 + P), \\ (\rho V)_{ij} = M_{ij}(\rho V) - \dfrac{\alpha^n_{ij}}{2S^n_{ij}}\Delta_{ij}(\rho UV), \end{cases} \tag{3.14}$$

where A_i is the area of cell c_i. The solution W^n_{ij} is recovered by using the following transformation

$$(\rho u)_{ij} = n_x(\rho U)_{ij} - n_y(\rho V)_{ij}$$

and

$$(\rho v)_{ij} = n_y(\rho U)_{ij} + n_x(\rho V)_{ij}.$$

4. Numerical results

4.1. 1D test problems

We introduce several numerical applications for Chaplygin gas model, to verify the performance and accurate of the NHRS scheme. The stability condition was chosen according to the following relation [18]

$$\Delta t = CFL\frac{\Delta x}{\max\limits_i\left(\left|\alpha^n_{i+\frac{1}{2}}S^n_{i+\frac{1}{2}}\right|\right)}, \tag{4.1}$$

constant CFL is to be chosen less than one. Indeed, the presented simulations depict the physical dynamical behaviour of solutions in the model of Chaplygin gas.

4.1.1. Test 1

We consider the first test case with the following initial conditions

$$(\rho, u) = \begin{cases} (3, 4) & \text{if} \quad x \leq 0, \\ (2, 6) & \text{if} \quad x > 0. \end{cases} \tag{4.2}$$

The domain $[-1, 1]$ is divided into 1000 gridpoints and the time of computation is $t = 0.05\ s$. The solution consists of two rarefaction waves. Figure 2 shows the numerical solution for density of gas and velocity utilizing NHRS, Rusanov, Lax-Friedrichs schemes and the reference solution computed with 20000 grid points. We note that the results obtained by NHRS scheme are more accurate than other schemes. The NHRS scheme grasp the shock and rarefaction waves in a very proper way. Figure 3 displays the change of parameter of control $\alpha^n_{i+\frac{1}{2}}$ and Riemann invariants.

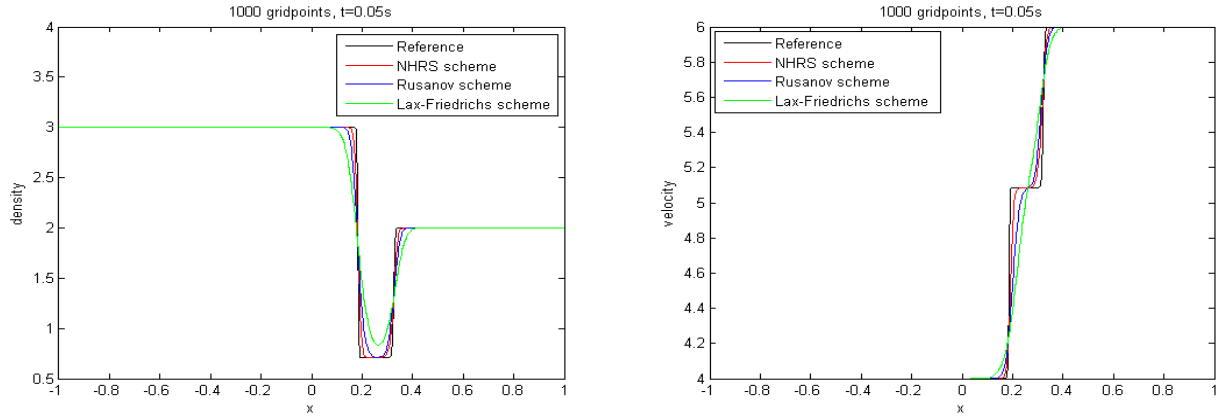

Figure 2. Density, velocity at t=0.05 s.

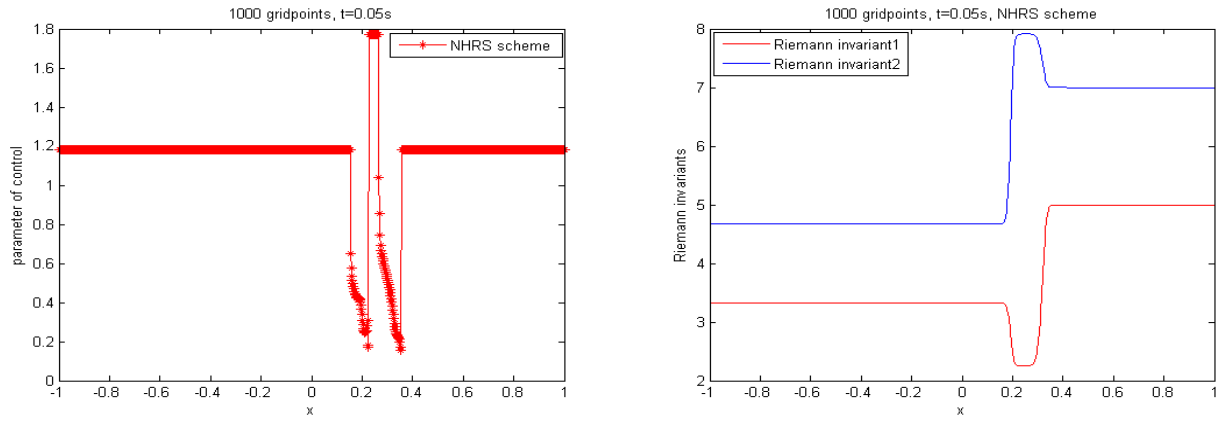

Figure 3. Parameter of control $\alpha^n_{i+\frac{1}{2}}$ and Riemann invariants at t=0.05 s.

4.1.2. Test 2

We consider the second test case with the following initial conditions

$$(\rho, u) = \begin{cases} (3, 4) & \text{if} \quad x \leq 0, \\ (6, 4) & \text{if} \quad x > 0. \end{cases} \tag{4.3}$$

The computational domain $[-1, 1]$ is divided into 1000 gridpoints and the time of computation is $t = 0.1\ s$. The solution consists of a 1-shock followed by a 2-rarefaction wave. Figure 4 illustrates the numerical solution for density and velocity, using NHRS, Rusanov, Lax-Friedrichs schemes and the reference solution computed with 20000 gridpoints. Figure 5 displays the change of parameter of control $\alpha^n_{i+\frac{1}{2}}$ and Riemann invariants.

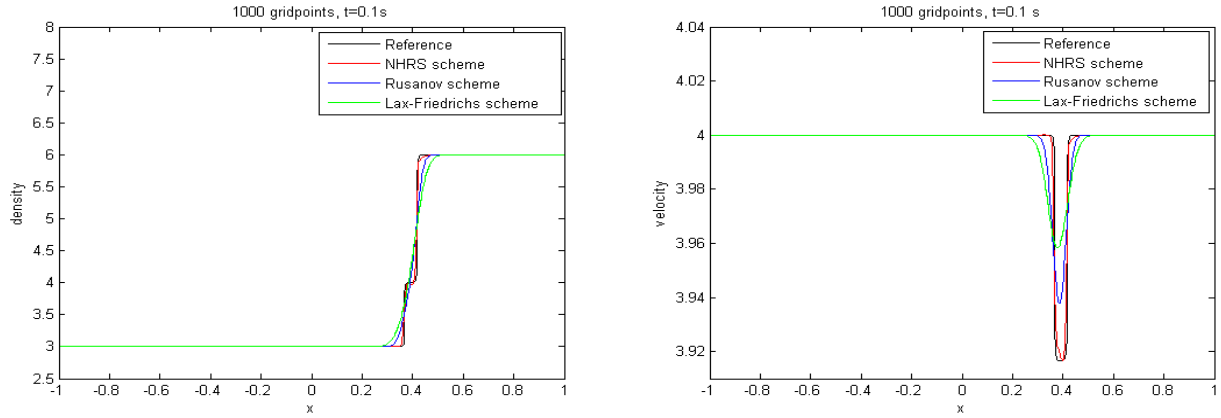

Figure 4. Density, velocity at t=0.1 s.

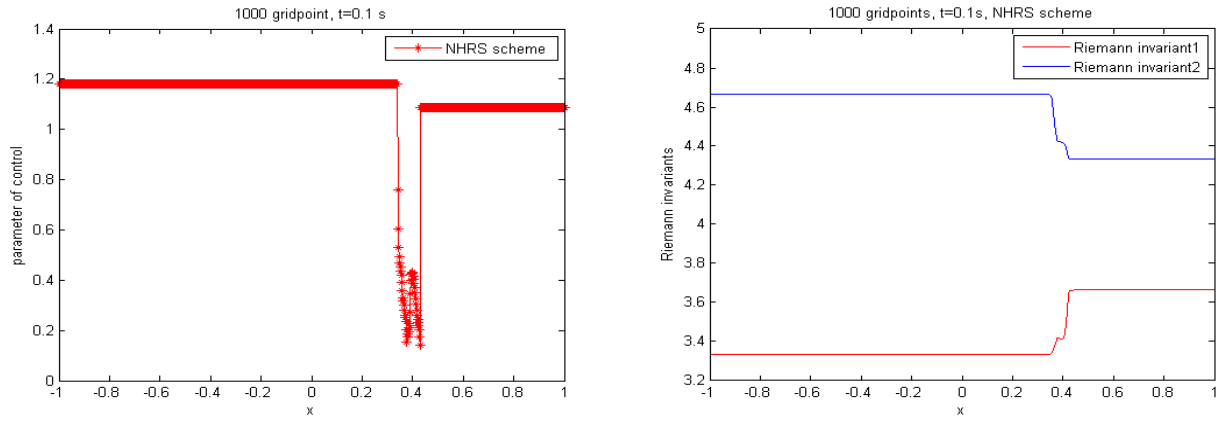

Figure 5. Parameter of control; Riemann invariants at t=0.1 s.

4.1.3. Test 3

We consider the third test case with the following initial conditions

$$(\rho, u) = \begin{cases} (3, 4) & \text{if} \quad x \leq 0, \\ (1, 4) & \text{if} \quad x > 0. \end{cases} \tag{4.4}$$

The solution consists of a 1-rarefaction wave followed by a 2-shock. Figure 6 displays the numerical solution for density and velocity using NHRS, Rusanov, Lax-Friedrichs schemes and the reference solution computed with 20000 grid points. Figure 7 shows the change of parameter of control $\alpha^n_{i+\frac{1}{2}}$ and Riemann invariants during computational time.

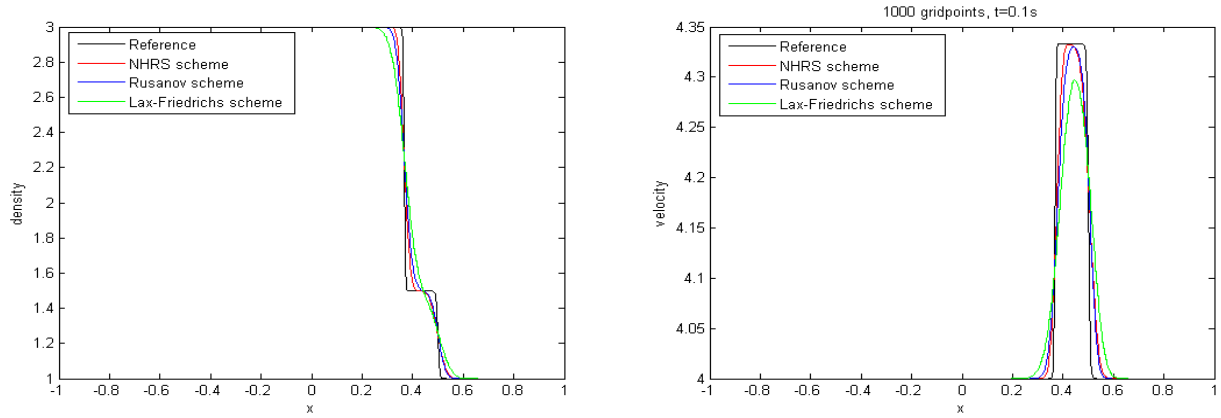

Figure 6. Density, velocity at t=0.1 s.

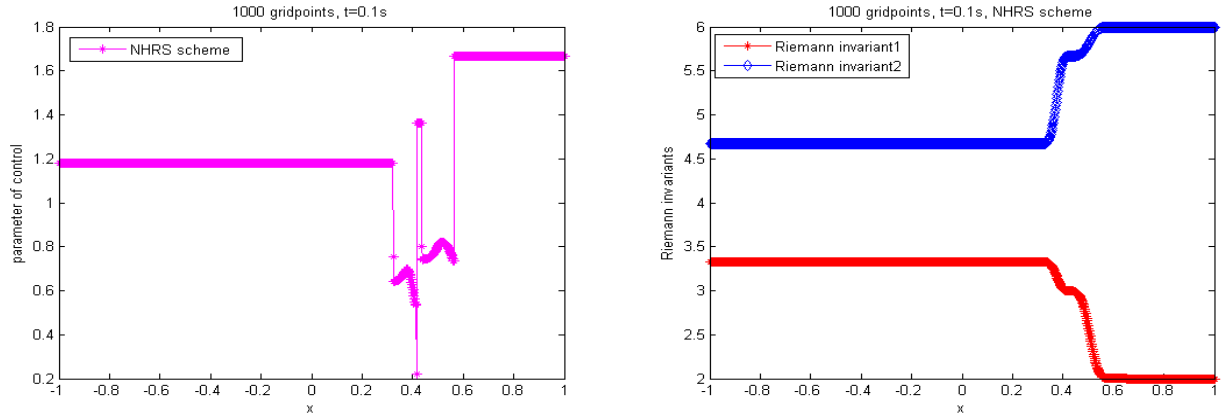

Figure 7. Parameter of control; Riemann invariants at t=0.1 s.

4.1.4. Test 4

We consider the fourth test case with the following initial conditions

$$(\rho, u) = \begin{cases} (0.4, 2) & \text{if} \quad x \leq 0, \\ (0.4, 0) & \text{if} \quad x > 0. \end{cases} \tag{4.5}$$

The solution consists of two shock waves. Figure 8 shows the numerical solution for density and velocity, using NHRS, Rusanov, Lax-Friedrichs schemes and the reference solution computed with 20000 gridpoints. Figure 9 shows the change of parameter of control $\alpha^n_{i+\frac{1}{2}}$ and Riemann invariants through computational time.

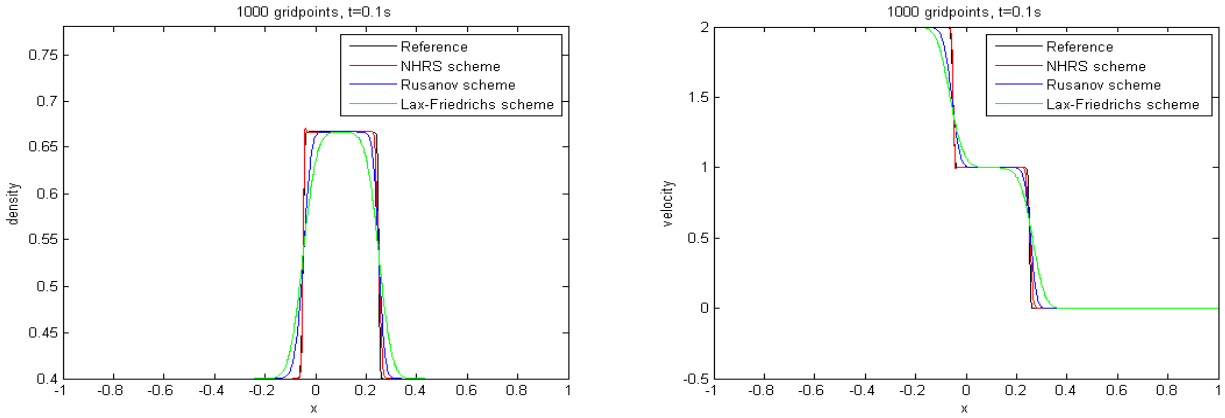

Figure 8. Density, velocity at t=0.1 s.

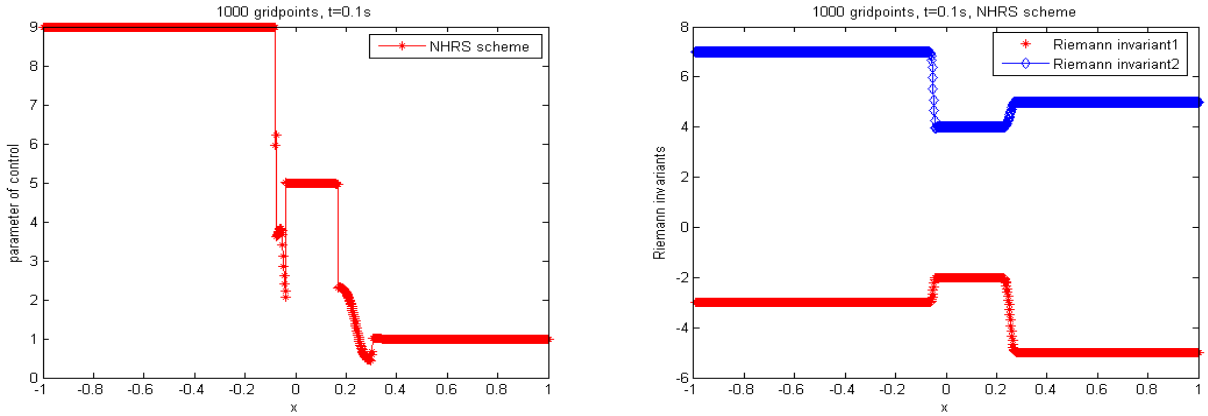

Figure 9. Parameter of control; Riemann invariants at t=0.1 s.

4.1.5. Test 5

We consider the fifth test case with the following initial conditions:

$$(\rho, u) = \begin{cases} (10, 0) & \text{if} \quad x \leq 0, \\ (1, 0) & \text{if} \quad x > 0. \end{cases} \tag{4.6}$$

The solution consists of a 1-rarefaction wave followed by a 2-shock. Figure 10 displays the numerical solution for density and velocity. Figure 11 shows the change of parameter of control, $\alpha^n_{i+\frac{1}{2}}$ and Riemann invariants through computational time.

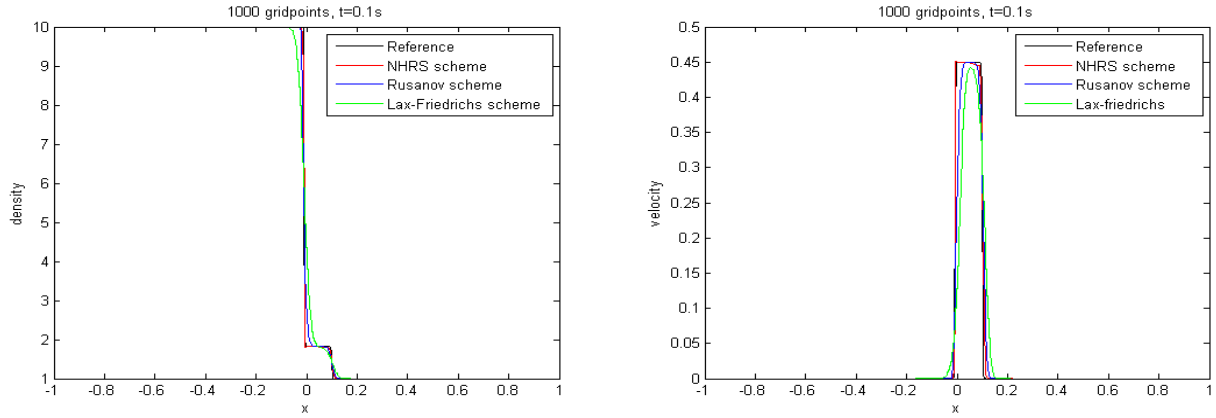

Figure 10. Density, velocity at t=0.1 s.

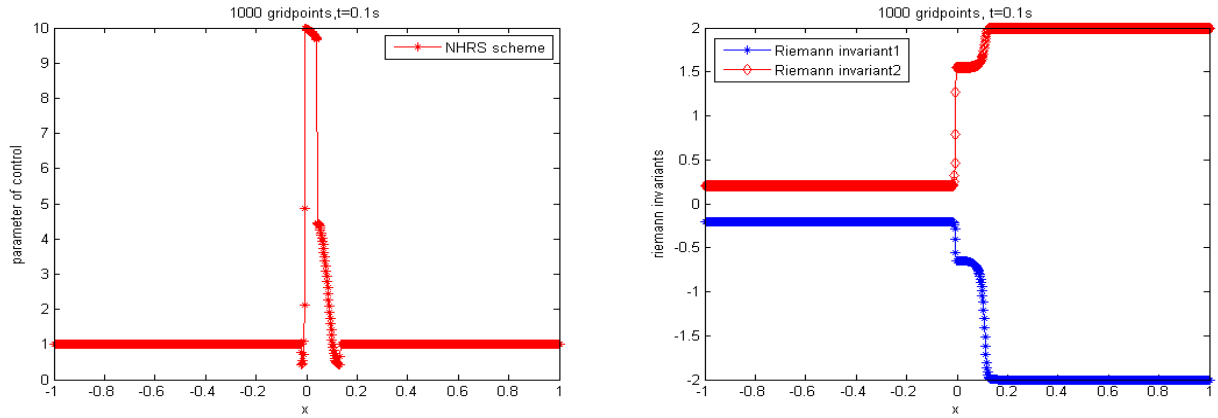

Figure 11. Parameter of control; Riemann invariants at t=0.1 s.

4.2. 2D test problems

Similar to 1D test cases, we present numerical results for a test problem to check the accuracy and the performance of the proposed finite volume method in two dimension. As with all explicit time stepping methods the theoretical maximum stable time step Δt is specified according to the CFL condition [18]

$$\Delta t \max_i \left(\frac{|\delta c_i|}{A_i} \right) \left[1 + \alpha \frac{M}{m} \right] \frac{M}{2} = Cr, \tag{4.7}$$

Cr is a constant to be chosen less than one. In all test cases, the fixed Courant number $Cr = 0.95$ is utilized and the time step is varied according to Eq (4.7), with $M = \max_{i,j}(S_{ij}^n)$ and $m = \min_{i,j}(s_{ij}^n)$, where S_{ij}^n is the local Rusanov velocity, A_i is the area of cell c_i , $\alpha = 1.2$ is the parameter of the scheme and $|\delta c_i|$ is the perimeter of a cell c_i.

4.2.1. Test 1

This test case consists of a 2D shock tube, it is of length 12 m and width is 1 m and the gate at $x_0 = 6$ m. The solution consists of two rarefaction waves. Figure 12 depicts the numerical solution for

density of gas and velocity utilizing NHRS where the initial condition is

$$(\rho, u, v) = \begin{cases} (3, 4, 0) & \text{if} \quad x \leq 6, \\ (2, 6, 0) & \text{if} \quad x > 6. \end{cases} \tag{4.8}$$

We simulate this case test with our numerical scheme at a final time $t = 0.753$ on unstructured grids $= 150 \times 15$. Figure 12 shows that the solution is similar the solution in 1D, and note that our scheme captures correctly the discontinuity and the shock without need of very fine mesh.

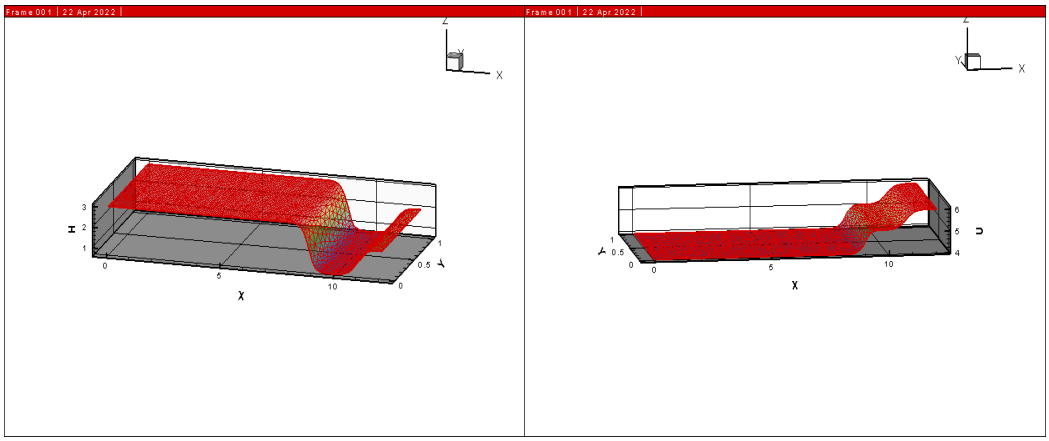

Figure 12. Numerical results of density and velocity at t=0.753 s, unstructure mesh= 150×15.

4.2.2. Test 2

This test case consists of a 2D shock tube, it is of length 12 m and width is 1 m and the gate at $x_0 = 6$ m. The solution consists of a 1-shock followed by a 2-rarefaction wave. Figure 13 illustrates the numerical solution for density of gas and velocity utilizing NHRS where the initial condition is

$$(\rho, u, v) = \begin{cases} (3, 4, 0) & \text{if} \quad x \leq 6, \\ (6, 4, 0) & \text{if} \quad x > 6. \end{cases} \tag{4.9}$$

We simulate this case test with our numerical scheme at a final time $t = 0.689$ on unstructured grids $= 150 \times 15$. Figure 13 shows that, the solution is similar the solution in one dimensional, and note that our scheme captures correctly the in one dimensional.

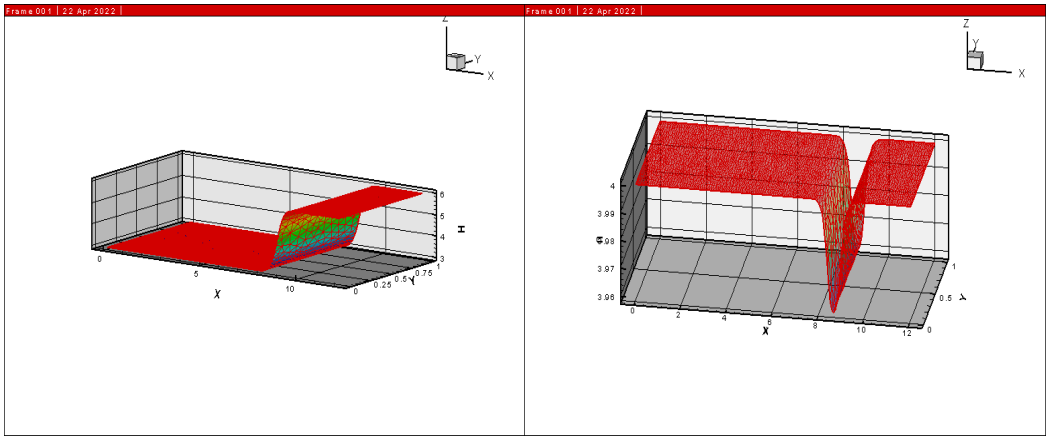

Figure 13. Numerical results of density and velocity at t=0.689 s, unstructure mesh= 150 × 15.

4.2.3. Test 3

This test case consists of a 2D shock tube, it is of length 12 m and width is 1 m and the gate at $x_0 = 6$ m. The solution consists of a 1-shock followed by a 2-rarefaction wave. Figure 14 illustrates the numerical solution for density of gas and velocity utilizing NHRS where the initial condition is

$$(\rho, u, v) = \begin{cases} (3, 4, 0) & \text{if} \quad x \leq 6, \\ \\ (1, 4, 0) & \text{if} \quad x > 6. \end{cases} \tag{4.10}$$

We simulate this case test with our numerical scheme at a final time $t = 0.75$ on unstructured grids = 150 × 15. Figure 14 shows that, the solution is similar the solution in 1D case.

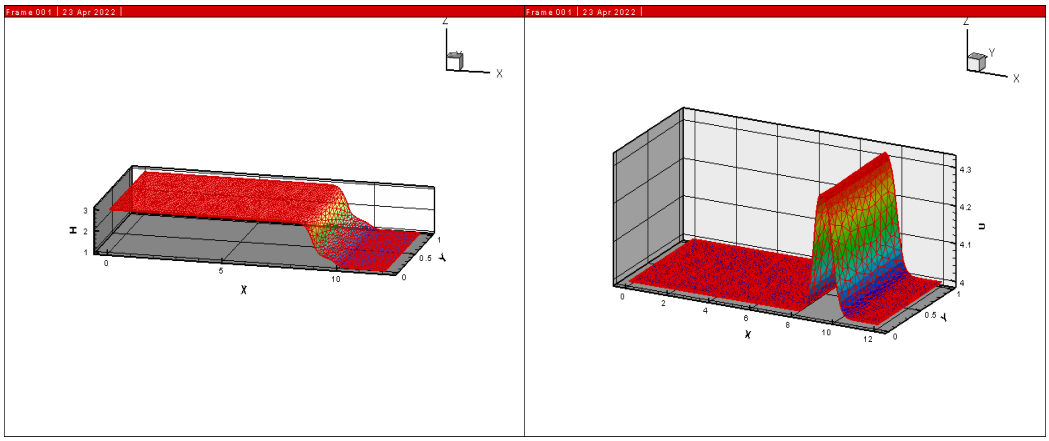

Figure 14. Numerical results of density and velocity at t=0.689 s, unstructure mesh= 150 × 15.

4.2.4. Test 4

This test case consists of a two dimensional shock tube, it is of length 12 m and width is 1 m and the gate at $x_0 = 6$ m, The solution consists of a 2-shock. Figure 15 shows the numerical solution for

density of gas and velocity utilizing NHRS where the initial conditions are given by

$$(\rho, u, v) = \begin{cases} (0.4, 2, 0) & \text{if} \quad x \leq 6, \\ \\ (0.4, 0, 0) & \text{if} \quad x > 6. \end{cases} \tag{4.11}$$

We simulate this case test with our numerical scheme at a final time $t = 0.544$ on unstructured grids, from Figure 15. we see that, the solution is similar the solution in one dimensional, and note that our scheme captures correctly the discontinuity and the shock without need of very fine mesh.

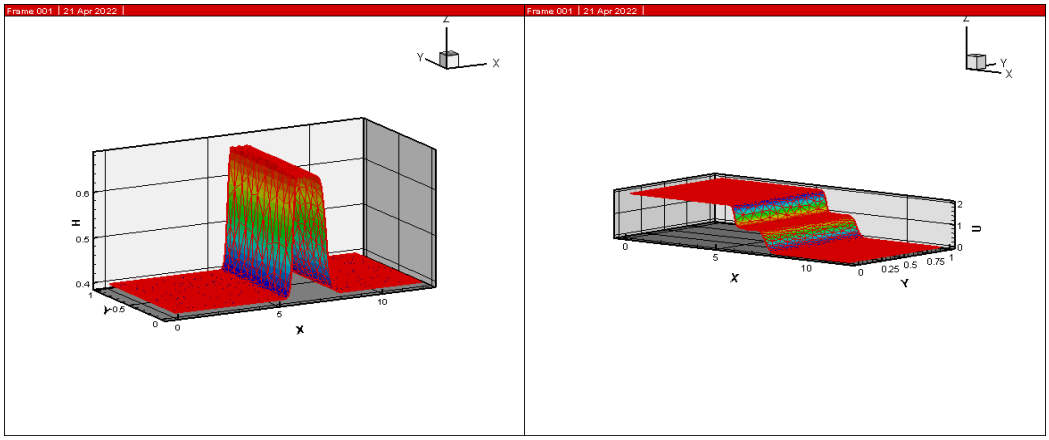

Figure 15. Numerical results of density and velocity at t=0.255 s, unstructure mesh= 150×15.

5. Conclusions

The NHRS scheme was applied to solve 1D and 2D Chaplygin gas model. The suggested scheme has capability to accurately capture the discontinues profiles of gas fluid and averts numerical diffusion in the solution. Several test cases are given in order to solve the Chaplygin gas model and compared with NHRS scheme, Rusanov scheme, modified Lax-Friedrichs and analytical solutions in 1D case. The presented simulations shown high resolution of NHRS technique and confirm its capability and efficiency to deal with such models.

Conflict of interest

The authors declare that they have no known competing financial interests or personal relationships that could have appeared to influence the work reported in this paper.

References

1. J. Smoller, *Shock waves and reaction-diffusion equations, Springer*, 1 Ed., 1994.
2. E. F. Toro, *Riemann solvers and numerical methods for fluid dynamics*, Springer, 1999.
3. M. A. E. Abdelrahman, Cone-grid scheme for solving hyperbolic systems of conservation laws and one application, *Comp. Appl. Math.*, **37** (2018), 3503–3513. https://doi.org/10.1007/s40314-017-0527-9

4. M. A. E. Abdelrahman, Global solutions for the ultra-relativistic Euler equations, *Nonlinear Anal.*, **155** (2017), 140–162. https://doi.org/10.1016/j.na.2017.01.014
5. M. A. E. Abdelrahman, On the shallow water equations, *Z. Naturforsch. A*, **72** (2017), 873–879. https://doi.org/10.1515/zna-2017-0146
6. S. Chaplygin, *On gas jets*, Scientific Memoirs, Moscow University Mathematic Physics, Vol. 21, 1904.
7. M. R. Setare, Holographic Chaplygin gas model, *Phys. Lett. B*, **648** (2007), 329–332. https://doi.org/10.1016/j.physletb.2007.03.025
8. Y. Brenier, Solutions with concentration to the Riemann problem for one-dimensional Chaplygin gas equations, *J. Math. Fluid Mech.*, **7** (2005), S326–S331. https://doi.org/10.1007/s00021-005-0162-x
9. L. H. Guo, W. C. Sheng, T. Zhang, The two-dimensional Riemann problelm for isentropic Chaplygin gas dynamic system, *Comm. Pure Appl. Anal.*, **9** (2010), 431–458. http://dx.doi.org/10.3934/cpaa.2010.9.431
10. Y. Hu, J. Q. Li, W. C. Sheng, Degenerate Goursat-type boundary value problems arising from the study of two-dimensional isothermal Euler equations, *Z. Angew. Math. Phys.*, **63** (2012), 1021–1046. https://doi.org/10.1007/s00033-012-0203-2
11. J. Q. Li, Y. X. Zheng, Interaction of four rarefaction waves in the bi-symmetric class of the two-dimensional Euler equations, *Commun. Math. Phys.*, **296** (2010), 303–321. https://doi.org/10.1007/s00220-010-1019-6
12. S. Chen, A. Qu, Two-dimensional Riemann problems for Chaplygin gas, *SIAM J. Math. Anal.*, **44** (2012), 2146–2178. https://doi.org/10.1137/110838091
13. G. Lai, W. C. Sheng, Y. X. Zheng, Simple waves and pressure delta waves for a Chaplygin gas in two-dimensions, *Discrete Contin. Dyn. Syst.*, **31** (2011), 489–523. https://doi.org/10.3934/dcds.2011.31.489
14. W. C. Sheng, T. Zhang, *The Riemann problem for transportation equations in gas dynamics*, Memoirs of the American Mathematical Society, Vol. 137, 1999. https://doi.org/10.1090/memo/0654
15. F. B. Li, W. Xiao, Interaction of four rarefaction waves in the bi-symmetric class of the pressure gradient system, *J. Differ. Equations*, **252** (2012), 3920–3952. https://doi.org/10.1016/j.jde.2011.11.010
16. K. Song, Y. X. Zheng, Semi-hyperbolic patches of solutions of the pressure gradient system, *Discrete Contin. Dyn. Syst.*, **24** (2009), 1365–1380. https://doi.org/10.3934/dcds.2009.24.1365
17. G. Q. Chen, X. M. Deng, W. Xiang, Shock diffraction by convex cornered wedges for the nonlinear wave system, *Arch. Rational Mech. Anal.*, **211** (2014), 61–112. https://doi.org/10.1007/s00205-013-0681-1
18. K. Mohamed, *Simulation numérique en volume finis, de problémes d'écoulements multidimensionnels raides, par un schéma de flux á deux pas*, Dissertation, University of Paris XIII, 2005.
19. K. Mohamed, M. Seaid, M. Zahri, A finite volume method for scalar conservation laws with stochastic time-space dependent flux function, *J. Comput. Appl. Math.*, **237** (2013), 614–632. https://doi.org/10.1016/j.cam.2012.07.014

20. F. Benkhaldoun, K. Mohamed, M. Seaid, A Generalized Rusanov method for Saint-Venant Equations with Variable Horizontal Density, In: J. Fořt, J. Fürst, J. Halama, R. Herbin, F. Hubert, *Finite volumes for complex applications VI problems & perspectives*, Springer Proceedings in Mathematics, Springer, Berlin, Heidelberg, **4** (2011), 89–96. https://doi.org/10.1007/978-3-642-20671-9_10
21. K. Mohamed, F. Benkhaldoun, A modified Rusanov scheme for shallow water equations with topography and two phase flows, *Eur. Phys. J. Plus*, **131** (2016), 207. https://doi.org/10.1140/epjp/i2016-16207-3
22. K. Mohamed, A finite volume method for numerical simulation of shallow water models with porosity, *Comput. Fluids*, **104** (2014), 9–19. https://doi.org/10.1016/j.compfluid.2014.07.020
23. K. Mohamed, A. R. Seadawy, Finite volume scheme for numerical simulation of the sediment transport model, *Int. J. Mod. Phys. B*, **33** (2019), 1950283. https://doi.org/10.1142/S0217979219502837
24. K. Mohamed, M. A. E. Abdelrahman, The modified Rusanov scheme for solving the ultra-relativistic Euler equations, *Eur. J. Mech. B/Fluids*, **90** (2021), 89–98. https://doi.org/10.1016/j.euromechflu.2021.07.014
25. S. Mungkasi, S. G. Roberts, A smoothness indicator for numerical solutions to the Ripa model, *J. Phys. Conf. Ser.*, **693** (2016), 012011. https://doi.org/10.1088/1742-6596/693/1/012011
26. S. J. Sherwin, L. Formaggia, J. Peiro, V. Franke, Computational modelling of 1D blood flow with variable mechanical properties and its application to the simulation of wave propagation in the human arterial system, *Int. J. Numer. Methods Fluids*, **43** (2003), 673–700. https://doi.org/10.1002/fld.543
27. P. Gupta, R. K. Chaturvedi, L. P. Singh, The generalized Riemann problem for the Chaplygin gas equation, *Eur. J. Mech. B/Fluids*, **82** (2020), 61–65. https://doi.org/10.1016/j.euromechflu.2020.03.001
28. R. J. LeVeque, *Numerical methods for conservation laws*, Birkhäuser Verlag Basel, Switzerland, 1992.
29. V. Rusanov, *Caculation of interaction of non-steady shock waves with obstacles*, National Research Council of Canada, Ottawa, 1961, 267–279.
30. P. K. Sweby, High resolution schemes using flux limiters for hyperbolic conservation laws, *SIAM J. Numer. Anal.*, **21** (1984), 995–1011. https://doi.org/10.1137/0721062
31. G. Wang, B. Chen, Y. Hu, The two-dimensional Riemann problem for Chaplygin gas dynamics with three constant states, *J. Math. Anal. Appl.*, **393** (2012), 544–562. https://doi.org/10.1016/j.jmaa.2012.03.017

AIMS Press